International Journal of Mineral Processing 156 (2016) 108–115

Contents lists available at ScienceDirect

International Journal of Mineral Processing

journal homepage: www.elsevier.com/locate/ijminpro

The effect of energy input on flotation kinetics

Mehdi Safari [a,*], Martin Harris [a], David Deglon [a], Laurindo Leal Filho [b], Francisco Testa [b]

[a] Centre for Minerals Research, Department of Chemical Engineering, University of Cape Town, Private Bag Rondebosch, Cape Town 7700, South Africa
[b] Department of Mining and Petroleum Engineering, University of São Paulo, São Paulo, Brazil

ARTICLE INFO

Article history:
Received 22 December 2015
Received in revised form 13 May 2016
Accepted 17 May 2016
Available online 18 May 2016

Keywords:
Flotation kinetics
Energy input
Particle size
Bubble size
Collector dosage
Oscillating grids

ABSTRACT

This paper investigates the effect of energy/power input on the flotation of three sulphide minerals (galena, pyrite & pentlandite) and three oxide minerals (apatite, hematite & quartz) in an oscillating grid flotation cell (OGC). Oscillating grids generate near ideal hydrodynamic environments, characterised by turbulence which is relatively homogeneous and isotropic. Galena, pyrite, pentlandite (−150 μm), apatite (−650 μm), hematite (−75 μm) and quartz (−75 μm) were floated in the OGC at power intensities from 0.1 to 5.0 W/kg, using 0.13, 0.24, 0.58 and 0.82 mm bubbles, and at three collector dosages. Results show that the effect of power intensity on the flotation rate is strongly dependent on the mineral type, particle size, bubble size and collector dosage. In general, fine particles benefit from higher energy inputs, intermediate particles have an optimum energy input, and coarse particles do not benefit from agitation.

1. Introduction

There is a considerable body of experimental and theoretical evidence to suggest that energy/power input plays an important role in flotation kinetics, particularly in the finer particle sizes where flotation efficiency is poor (Deglon, 2005). A number of excellent studies into the effect of energy on flotation kinetics have been carried out in impeller stirred cells (Ahmed and Jameson, 1985; Deglon, 2002; Pyke et al., 2003; Newell and Grano, 2006). Investigations using this type of cell have a number of limitations. The impeller influences particle suspension, bubble break-up and agitation in the cell. In addition, turbulence is highly inhomogeneous and anisotropic, with power intensities near the impeller orders of magnitude higher than those found elsewhere in the cell (Deglon, 1998; Koh and Schwarz, 2003; Schubert, 1999, 2008). These limitations have resulted in the development of novel cells for the investigation of energy input.

Anderson et al. (2009) developed a novel oscillating baffled cell (OBC) which had the benefit of decoupling solid suspension, bubble generation and energy input. It was found that the unique bulk oscillatory motion of the fluid in the cell had a strong effect on flotation kinetics at very low power intensities. This cell has potential for industrial applications but is limited as a research tool due to the complex nature of the fluid flow. Changunda et al. (2008) used a novel oscillating grid cell (OGC), based on the design of Bache and Rasool (2001), to investigate the effects of energy input on flotation kinetics. The OGC decouples the processes of solid suspension and bubble generation as well as producing relatively homogeneous and isotropic turbulence. Due to the near ideal nature of the turbulence generated, oscillating grids have been used in many areas of research including mixing across density layers (McDougall, 1979), combustion (De-Silva and Fernando, 1994), sedimentation (Huppert et al., 1995), coagulation (Brunk et al., 1998), resuspension (Orlins and Gulliver, 2003), precipitation (Mokgethi, 2010), turbulence and the gas transfer processes (Herlina and Jirka, 2008). Oscillating grids provide a potentially ideal environment for investigating the effects of energy input on flotation kinetics, which cannot be achieved in impeller stirred cells. The work of Changunda et al. (2008) was however limited to relatively low power intensities (<0.60 W/kg). Massey et al. (2012) used the design of Changunda et al. (2008) to develop an oscillating grid flotation cell capable of operating at high power intensities of up to 5 W/kg. Massey et al. (2012) conducted a preliminary study on the flotation of quartz at a single collector dosage. The aim of this study is to investigate the effect of energy/power input on the flotation of three sulphide minerals (galena, pyrite & pentlandite) and three oxide minerals (apatite, hematite & quartz), with three different bubble sizes and at three collector dosages, in an oscillating grid flotation cell (OGC). To the authors' knowledge, this study consisting of over 400 flotation tests represents the most comprehensive investigation of the effect of energy/power on flotation kinetics in a relatively homogeneous and isotropic turbulent environment.

2. Energy input in flotation

2.1. Theoretical findings

Energy input (or agitation) is considered to influence all of the sub processes of flotation, either directly or indirectly through bubble

* Corresponding author.
E-mail address: SFRMEH001@Myuct.ac.za (M. Safari).

http://dx.doi.org/10.1016/j.minpro.2016.05.008
0301-7516/

breakup and particle dispersion. Models for turbulent collision suggest that the rate of flotation is proportional to the power intensity, or turbulent energy dissipation rate, to the power of between 0.50 and 0.75 (Deglon, 2002). The majority of theoretical studies suggest that agitation increases the rate of particle-bubble collision, which is especially important for fine particles (Saint Amand, 1999; Schubert, 1999). It is unclear whether agitation improves particle-bubble attachment due to conflicting results as to the effect of agitation on particle-bubble contact time. However, studies suggest that agitation helps to overcome the 'energy barrier' to attachment. All studies conclude that agitation significantly increases particle-bubble detachment for coarser particles but has a lesser influence on fine particles. Here, the destabilizing influence (probability of detachment, stress on aggregate, detachment force) has been shown to be proportional to the power intensity to the power of between 0.66 and 1.0 (Deglon, 2002). Several studies have combined the various theoretical models for particle-bubble collision, attachment and detachment in simulations of agitated flotation cells (Saint Amand, 1999; Koh and Schwarz, 2003; Pyke et al., 2003; Sherrell and Yoon, 2005). These studies demonstrate that agitation generally increases the rate of flotation of finer particles, as noted in numerous studies by Schubert (1999).

2.2. Experimental findings

Over the past few decades there have been numerous studies where flotation rates/recoveries have been investigated as a function of agitation, particle size, particle density and bubble size. Practically all of these studies have demonstrated that increasing agitation improves the rate of flotation of fine particles (Schubert and Bischofberger, 1978; Ahmed and Jameson, 1985; Jordan and Spears, 1990; Deglon, 2002; Pyke et al., 2003; Newell and Grano, 2006, Schubert, 2008). The majority of these studies have been for normal flotation bubbles and the few studies on microbubbles have found that far lower levels of agitation are required for optimum flotation (Ahmed and Jameson, 1985; Deglon, 2002). Some studies have attempted to quantify the increase in the rate of flotation with increasing agitation. Nonaka et al. (1982); Saint Amand (1999) and Deglon (2002) found that the rate of flotation increases with the power intensity to the power of 0.75, 0.50 and 0.91 respectively. Newell and Grano (2006) and Changunda et al. (2008) found a near linear increase in the rate of flotation with increasing power intensity. Massey et al. (2012) showed that the effect of power intensity on flotation kinetics is strongly dependent on both particle and bubble size.

3. Experimental

3.1. Oscillating grid flotation cell

A schematic of the oscillating grid cell and physical specifications of the cell and grids are given in Fig. 1. The grids were cut from a single sheet of 1.5 mm stainless steel for added strength. Nineteen grids were mounted horizontally on the drive shaft to make up the grid stack. The turbulence was generated in the cell by oscillating the grid stack at a set stroke length of 18 mm, which corresponds to the spacing between the grids. The power intensity was altered by changing the oscillating frequency which was manipulated by changing the rotational speed of the motor. A recycle was used to continuously circulate particles through the cell. Nitrogen gas was used in the study and was saturated by bubbling it through distilled water before being sparged into the cell through three 30 mm diameter sintered glass discs (Duran, supplied by Glasstech Pty. Ltd.) situated below the grid stack. Porosity 1, 2 and 4 discs were used which produced bubble sizes of 0.82 mm, 0.58 mm and 0.13 mm (Deglon, 2002). The gas flow rate was accurately controlled by using a Brookes Smart (TMF) mass flow controller. In order to minimise froth recovery effects the concentrate was manually suctioned from the surface, a technique used by previous researchers (Ahmed and Jameson, 1985; Deglon, 2002, Changunda et al., 2008; Massey et al., 2012).

The average power intensity was determined by measuring the force which was supplied to the system using a load cell (Loadcell Services S-type load cell) mounted in line with the drive shaft. The force exerted on the fluid by the grids (F) was calculated by measuring the force applied to the drive shaft with and without fluid in the cell. An optical sensor on the drive shaft was used to determine the frequency and phase of the drive shaft. A national instruments data acquisition card was used for measuring electrical signals and LabView© for signal analysis. The average power input was calculated from the integral of the power over one oscillation (Tojo et al., 1979):

$$\overline{P} = \int_0^{1/f} F_D(t)v(t)dt \quad (1)$$

where F is the instantaneous measured force, v is velocity of the grid stack, and f is the oscillating frequency. The average power intensity was calculated as (Schubert, 1999):

$$\varepsilon = \frac{\overline{P}}{m_L} \quad (2)$$

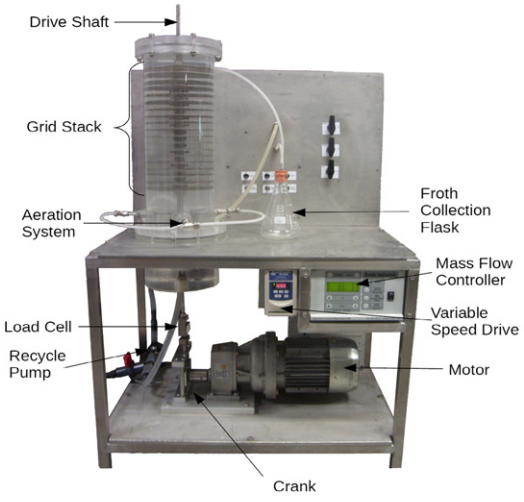

Laboratory OGC	Dimension
Volume	0.01 m^3
Tank height	0.38 m
Tank diameter	0.18 m
Number of grids	19
Mesh size	0.0068 m
Grid spacing	0.018 m
Bar diameter	0.0016 m

Fig. 1. The oscillating grid flotation cell and cell specifications.

where m_L is the mass of the fluid being agitated. It should be noted that under the conditions used in the investigation, expressing energy/power input as power intensity (kW/m^3), specific power input (W/kg) or turbulent energy dissipation rate (W/kg or m^2/s^3) is equivalent.

3.2. Materials and reagents

Flotation experiments were performed in the oscillating grid cell using three sulphide minerals (galena, pyrite and pentlandite) and three oxide minerals (apatite, hematite and quartz). Galena (PbS) originated from the Touissit mine, Morocco. Pyrite (FeS_2) was obtained from the Huanzala Mine, Peru. Pentlandite ($(Fe,Ni)_9S_8$) was obtained from the Frood-Stobie Mine, Canada. Apatite ($Ca_5(PO_4)_3F$) was obtained from the Ipiá Mine, Brazil. Hematite (Fe_2O_3) was obtained from the Timbopeba Mine, Brazil. Quartz (SiO_2) was supplied by Kiln Contracts (Pty) Ltd., South Africa. Minerals were crushed, pulverized, sealed in plastic bottles and polyethylene bags and stored under nitrogen at −30° C to minimise oxidation. Mineralogical and X-ray powder diffraction data indicated that the all samples were of high purity with no impurity peaks detected. The elemental composition of the minerals was determined by ICP analysis. The specific gravity of the minerals was determined using a pycnometer. BET analysis was used to determine the specific surface area of the samples using a Micromeritics TriStar II 3020. QEMSCAN images showed that particles were generally angular in shape. The bulk elemental composition, specific gravity and specific surface area of samples are shown in Table 1.

Xanthates (SEX — sodium ethyl xanthate, PAX — potassium ethyl xanthate, SIBX — sodium isobutyl xanthate) were received in powder form and used as collectors for sulphide minerals. Fatty amines or acids (DAC — dodecyl amine chloride, EDA — ether dodecyl amine, OA — oleic acid) were received in liquid form and used as collectors for oxide minerals. MIBC (methyl isobutyl carbinol) was used as a frother. Reagents were prepared on a daily basis and adjusted to the correct pH using NaOH and HCl, if required. All reagents were of the analytical grade quality. All solutions were made with deionized water.

3.3. Experimental conditions and procedures

The conditions for the flotation experiments are given in Table 2. A low gas flow rate and mass percentage solids were used to have minimal influence on turbulence in the oscillating grid cell. Power intensities were chosen to cover the range of typical values found in industrial mechanical flotation cells. Bubble sizes are small in terms of industry use; however correspond to the range typically used by researchers. A high frother dosage was used to minimise bubble coalescence in the system. A range of short chain collectors (SEX, PAX, SIBIX) and long chain collectors (DAC, EDA, OA) were used for sulphide and oxide minerals respectively. Collector dosage was calculated as a percentage of mono-layer surface coverage. During the flotation experiments, six concentrates were collected at the times specified in Table 2. Samples were filtered and dried before sizing using a Malvern Mastersizer™ 2000. The mass recovery of each size class was calculated and used to determine the flotation rate constant using the standard first-order expression for a batch flotation cell. Entrainment was assumed to be negligible due to the low percentage solids and water recovery. A summary of the experimental flotation test for all samples is given in Table 3. Repeatability was determined by performing duplicate flotation experiments for all conditions. The average relative error (coefficient of variation) on the flotation rate constant was found to be around 6%.

Table 2
Experimental conditions for flotation tests.

Condition/parameter	Value (sulphide minerals)	Value (oxide minerals)
Solids	Galena, pyrite, pentlandite	Apatite, hematite, quartz
Solids concentration (mass %)	0.5	0.5
Gas	Nitrogen	Nitrogen
Superficial gas velocity (cm/s)	0.0065	0.0065
Bubble size (mm)	0.13, 0.58, 0.82	0.13, 0.24, 0.58, 0.82
Particle size (μm)	−150	−650, −75, −75
Energy input (W/kg or kW/m^3)	0.5, 1, 2, 3	0.1, 0.5, 1, 2, 3, 4, 5
Sampling time (min)	1, 2, 3, 4, 6, 9	1, 2, 3, 4, 6, 9
Frother	MIBC	MIBC
Frother concentration (ppm)	100	100
Collector	SEX, PAX, SIBX	OA, DAC, EDA
Collector dosage	Low, moderate, high	Low, moderate, high
Surface coverage	25%, 50%, 100%	25%, 50%, 100%

Note: Oxide minerals were floated at selected conditions from those given in the table.

4. Results and discussion

This section presents and discusses results for the effect of energy input on the flotation rate constant for the three sulphide minerals (galena, pyrite & pentlandite) and the three oxide minerals (apatite, hematite & quartz). The focus of the study was on the flotation of sulphide minerals. Here, results are presented for three particle size classes (fine, intermediate, coarse), as a consistent size distribution was used for all three minerals. For oxide minerals, results are presented by mineral type (apatite, hematite & quartz) as different size distributions and test conditions were used for the minerals, due to the nature of oxide flotation e.g. apatite is a coarser float than hematite. It should be noted that the relative magnitude of the flotation rate constant depends quite strongly on the mineral type. So for example, in general galena has significantly higher flotation rate constants than hematite. Thus results are discussed in terms of trends in the flotation rate constant, rather than the overall magnitude.

4.1. Sulphide minerals

This section presents and discusses results for the galena, pyrite and pentlandite flotation tests. Flotation results are divided into three particle size classes for comparative purposes, namely, −19 μm (fine), +19–38 μm (intermediate) and +38–150 μm (coarse). Galena, pyrite and pentlandite flotation results are indicated as “A”, “B” and “C” respectively on all figures.

Table 1
Specific gravity, specific surface area and bulk elemental composition of mineral samples.

Mineral	Specific gravity	BET	Elements present (mass percentage)									
Unit/elements	g/cm^3	m^2/g	S	Fe	Pb	Cu	Zn	Ca	Mg	Si	P	Ni
Pyrite	5.07	0.51	53.52	45.61	0.04	0.12	0.20	0.07	0.01	0.16	0.10	0.01
Galena	7.60	0.21	13.12	0.07	86.11	0.05	0.01	0.02	0.23	0.09	0.15	0.01
Pentlandite	4.42	1.07	32.5	34.56	0.04	0.84	0.05	0.41	0.52	2.07	0.12	27.32
Apatite	3.19	0.11	0.00	0.01	0.00	0.00	0.00	39.36	0.00	0.02	18.25	0.00
Hematite	5.30	2.47	0.00	49.16	0.00	0.00	0.00	0.01	0.00	13.95	0.00	0.00
Quartz	2.65	0.17	0.00	0.01	0.00	0.00	0.00	0.01	0.01	46.55	0.00	0.00

Table 3
Summary of flotation tests.

Summary	Sulphide minerals			Oxide minerals		
	Galena	Pyrite	Pentlandite	Apatite	Hematite	Quartz
Number of tests	137	85	122	71	21	27
Number of repeats	3.81	2.36	3.39	1.97	1.50	1.28
Relative error (k) %	6.73	5.93	6.31	8.47	3.60	5.67
Number of mass balance analysis	959	595	854	497	84	126
Number of BET tests	25	19	17	7	3	3

4.1.1. Fine particles

Fig. 2 shows the relationship between the flotation rate constant and the energy/power input for the fine particles (−19 μm) and for all bubble sizes and collector dosages. The flotation rate constant increases with increasing collector dosage, which is to be expected. This is attributed to an increase in the probability of bubble-particle attachment (Pushkarova and Horn, 2008). The flotation rate constant increases significantly with decreasing bubble size. This is due to an increase in the probability of bubble-particle collision for smaller bubbles, which is well established in the flotation literature for both

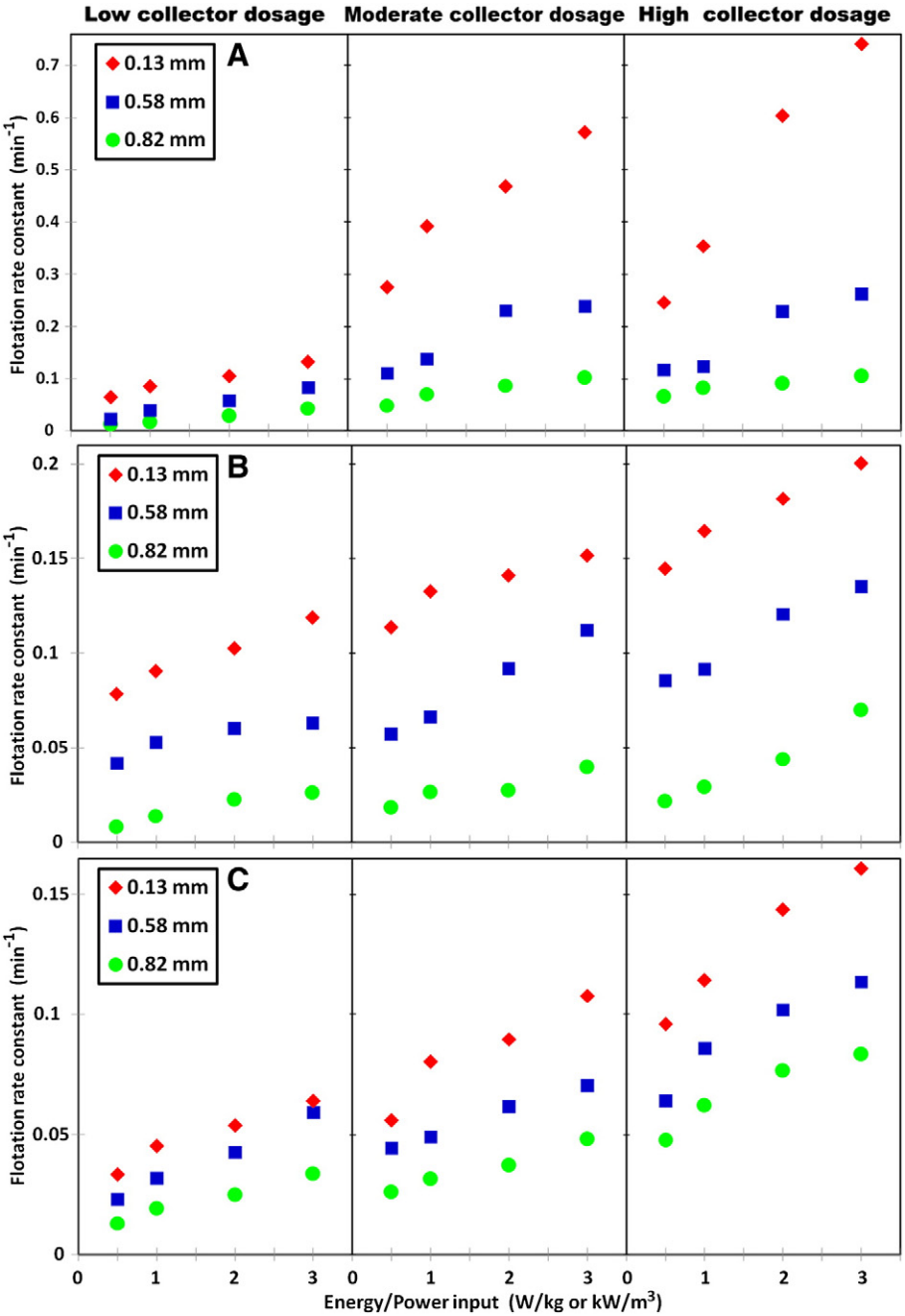

Fig. 2. Flotation rate constant versus energy input for the flotation of fine particles (−19 μm), all bubble sizes and collector dosages, A: galena, B: pyrite, C: pentlandite.

quiescent systems (Yoon and Luttrell, 1986; Diaz-Penafiel and Dobby, 1994, Nguyen et al., 2006) and turbulent systems at low power intensities (Ahmed and Jameson, 1985; Deglon, 2002; Changunda et al., 2008, Massey et al., 2012). For example, for galena at a moderate collector dosage and high energy input, the flotation rate constant increases by over 500% with a decrease in bubble size from 0.82 to 0.13 mm. The flotation rate constant increases steadily with increasing energy input for all bubble sizes and collector dosages. Here, increases of up to 300% are observed when increasing energy input from 0.5 to 3 W/kg. This significant increase suggests that energy input improves the flotation of fine particles, as observed in numerous theoretical and experimental studies (Schubert and Bischofberger, 1978; Ahmed and Jameson, 1985; Jordan and Spears, 1990; Deglon, 2002; Pyke et al., 2003; Newell and Grano, 2006; Schubert, 2008; Massey et al., 2012). This is primarily attributed to an increase in the number of bubble-particle collisions.

4.1.2. Intermediate particles

Fig. 3 shows the relationship between the flotation rate constant and the energy/power input for the intermediate particles (+19–38 μm) and for all bubble sizes and collector dosages. The intermediate particles have flotation rates which are generally larger than those for fine particles, at the lower energy inputs. This is due to an increase in the probability of bubble-particle collision for larger particles and is well established in the flotation literature (Ahmed and Jameson, 1985; Deglon, 2002; Pyke et al., 2003; Changunda et al., 2008; Anderson et al., 2009; Massey et al., 2012). Again the flotation rate constant increases with increasing collector dosage and decreasing bubble size. For intermediate galena particles, increasing energy input has no effect on the flotation rate constant at the low collector dosages but leads to an optimum in the flotation rate constant at both moderate and high collector dosages. This optimum is at around 1 W/kg for the moderate collector dosage and 2 W/kg for the high collector dosage, with subsequent

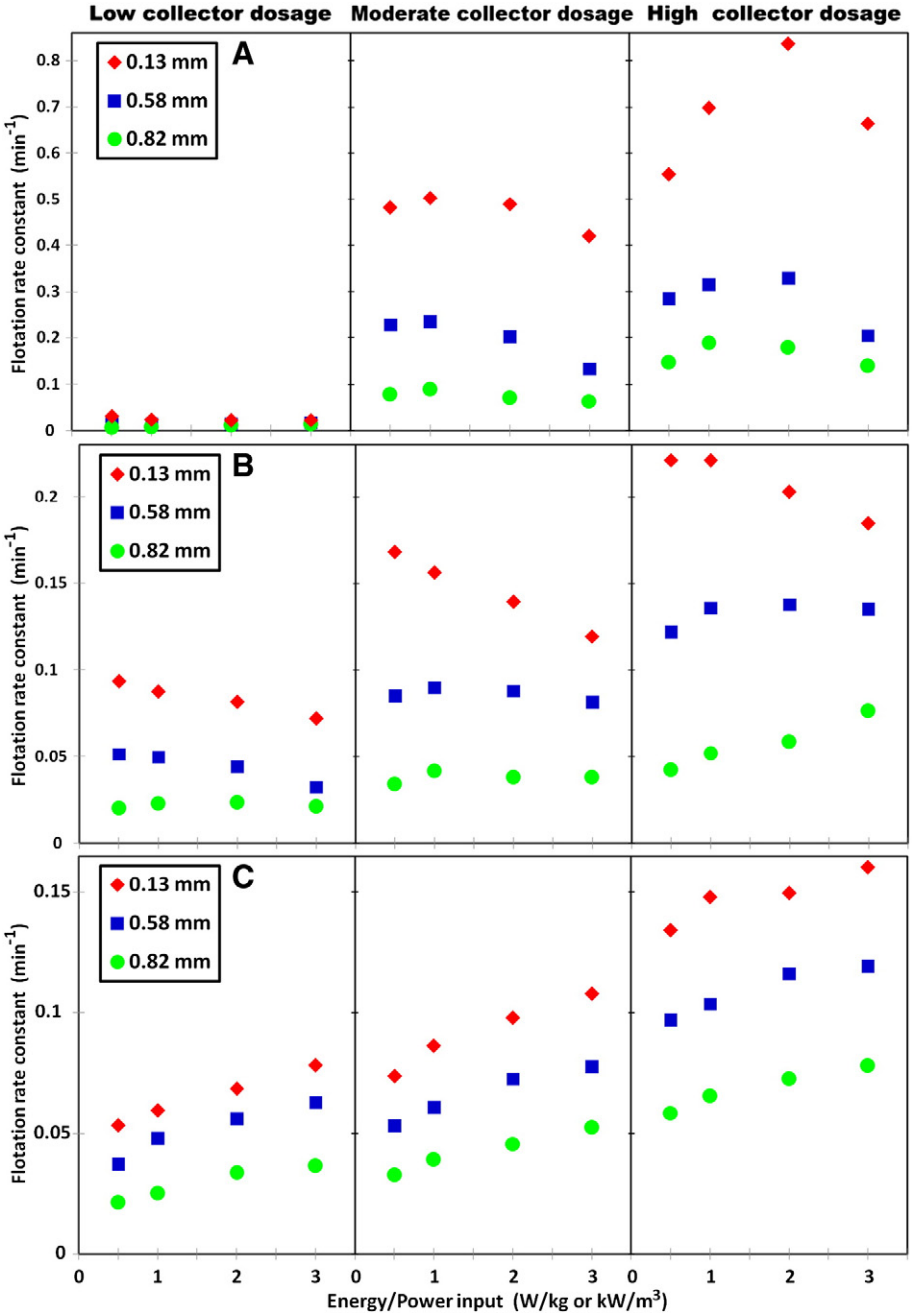

Fig. 3. Flotation rate constant versus energy input for the flotation of intermediate particles (+19–38 μm), all bubble sizes and collector dosages, A: galena, B: pyrite, C: pentlandite.

increases in the energy input resulting in large decreases in flotation rates for all bubble sizes. For intermediate pyrite particles, increasing energy input generally leads to a decrease in the flotation rate constant for small bubble sizes and a slight increase, or a shallow optimum, for intermediate and large bubble sizes. For intermediate pentlandite particles, increasing energy input generally leads to an increase in the flotation rate constant, although results tend towards a shallow optimum at the higher energy inputs. The intermediate galena particles probably have a much sharper optimum at lower energy inputs due to the higher particle density, resulting in increased bubble-particle detachment. A similar argument could apply when comparing the pyrite and pentlandite results, although the density difference is much smaller.

4.1.3. Coarse particles

Fig. 4 shows the relationship between the flotation rate constant and the energy/power input for the coarse particles (+38–150 μm) and for all bubble sizes and collector dosages. It is clear from this figure that increasing energy input leads to large decreases in the flotation rate constant for all bubble sizes and collector dosages. This is due to an increase in the probability of bubble-particle detachment for larger particles, as a result of increased turbulence, which reduces the stability of coarse bubble-particle aggregates (Schulze, 1993; Öteyaka and Soto, 1995; Cowburn et al., 2006). For example, for galena at a high collector dosage and small bubble size, the flotation rate constant decreases by over 400% as the energy input increases from 0.5 to 3 W/kg. The comparative decrease is around 300% for pyrite and 200% for pentlandite, which is significantly smaller than that for galena. As indicated previously, this is probably due to the much higher particle density for galena, resulting in increased bubble-particle detachment. It is also clear from this figure that detachment increases with decreasing bubble size. For example, at a high collector dosage and 0.5 W/kg energy input, the flotation rate constant for the small bubble size is 230% greater than that for the

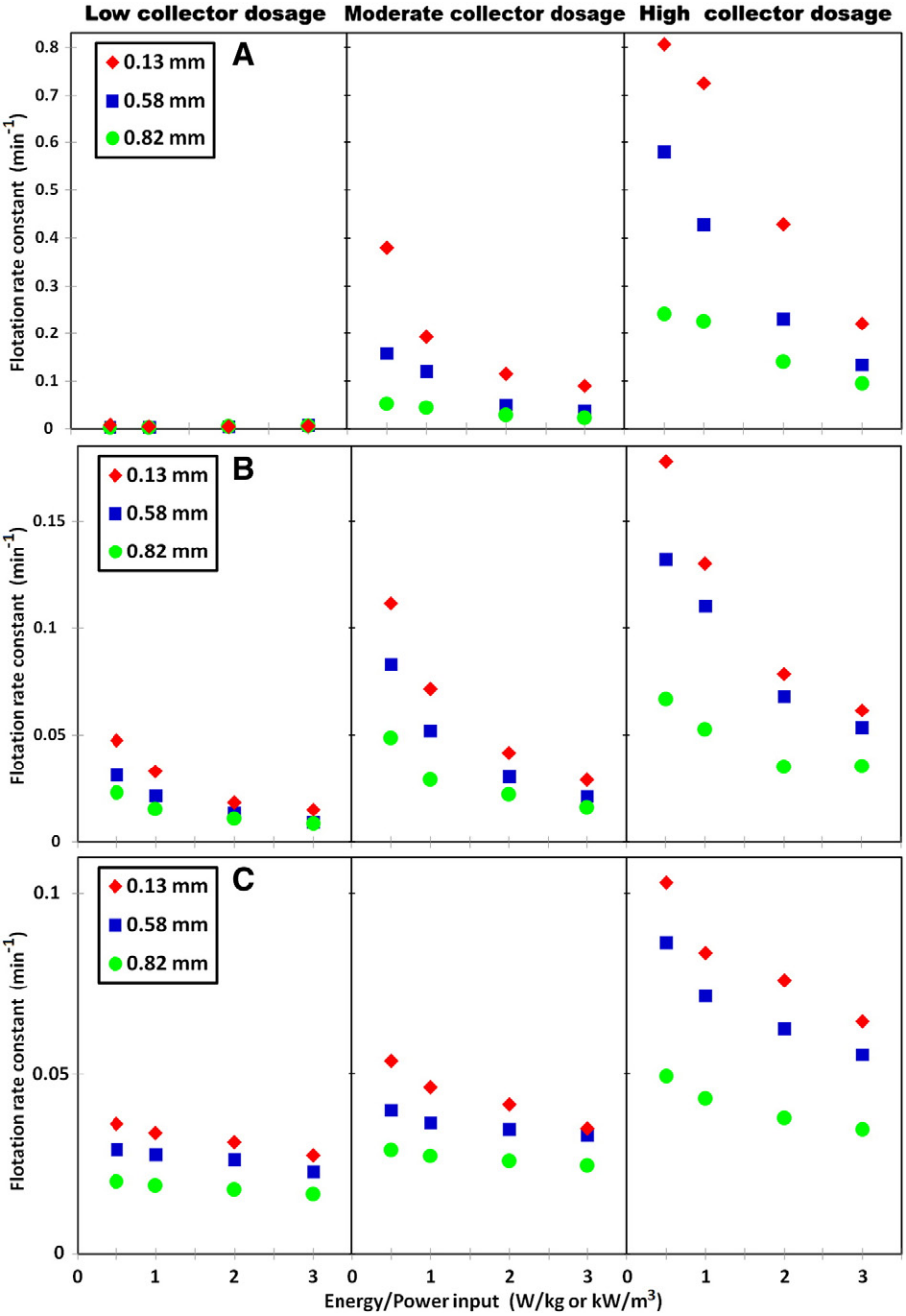

Fig. 4. Flotation rate constant versus energy input for the flotation of coarse particles (+38–150 μm), all bubble sizes and collector dosages, A: galena, B: pyrite, C: pentlandite.

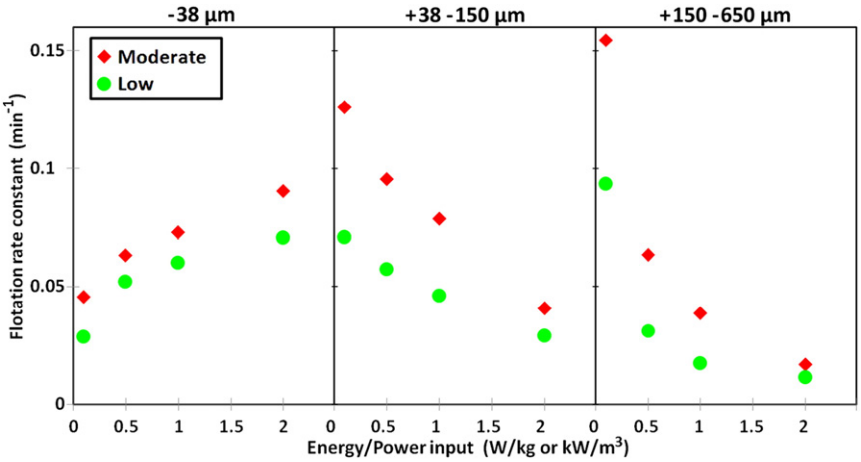

Fig. 5. Flotation rate constant versus energy input for three particle size classes, 0.58 mm bubbles and two collector dosages.

large bubble size. However, this difference decreases to only 150% greater when the energy input is increased to 3 W/kg. This increase in bubble-particle detachment with decreasing bubble size has been observed by a number of researchers (Ahmed and Jameson, 1985; Deglon, 2002; Massey et al., 2012) and is sometimes attributed to increased acceleration of bubble-particle aggregates in the more vigorous smaller turbulent eddies.

4.2. Oxide minerals

This section presents and discusses results for the apatite, hematite and quartz flotation tests. As indicated previously, results are presented by mineral type as different size distributions and test conditions were used for the minerals, due to the nature of oxide flotation. Here, results are presented according to size classes appropriate to the mineral e.g. apatite is coarser than hematite. It should be noted that the majority of trends observed in the oxide mineral results are entirely consistent with those for the sulphide minerals. Hence this section presents a brief overview of key features, rather than a detailed description of the variation of the flotation rate constant with energy input, particle size, bubble size and collector dosage.

4.2.1. Apatite

Fig. 5 shows the relationship between the flotation rate constant and the energy/power input for three particle size classes, 0.58 mm bubbles and two collector dosages. Here, the apatite flotation results are for coarser particles at lower energy inputs. The flotation rate constant for the finer particles (−38 µm) increases by around 200% with an increase in energy input from 0.1 to 2 W/kg. However, the flotation rate constant for the very coarse particles (+150–650 µm) decreases by over 900% over the same energy input range. These results clearly demonstrate that optimal energy inputs for the flotation of fine and coarse apatite differ significantly, due to the wide particle size range found in most industrial flotation applications.

4.2.2. Hematite

Fig. 6 shows the relationship between the flotation rate constant and the energy/power input for two particle size classes, all bubble sizes and a moderate collector dosage. Here, the flotation rate constant increases steadily with increasing energy input for finer particles (−38 µm), but generally decreases for the slightly coarser particles (+38–45 µm). These results suggest that higher energy inputs are beneficial for the flotation of hematite, which consists predominantly of finer particles in most industrial flotation applications.

4.2.3. Quartz

Fig. 7 shows the relationship between the flotation rate constant and the energy/power input for three particle size classes, all bubble sizes and a moderate collector dosage. The trends in this figure tend to mirror those observed in Figs. 2 to 4 for the sulphide minerals with the exception that, for the small bubbles, increasing energy input does not

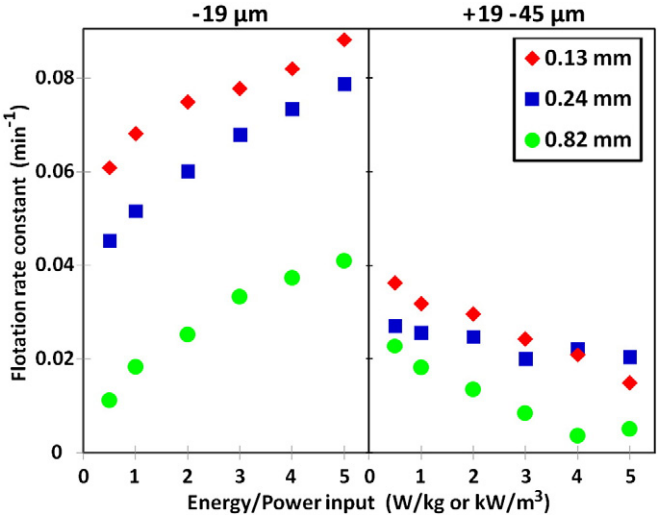

Fig. 6. Flotation rate constant versus energy input for two particle size classes, all bubble sizes and a moderate collector dosage.

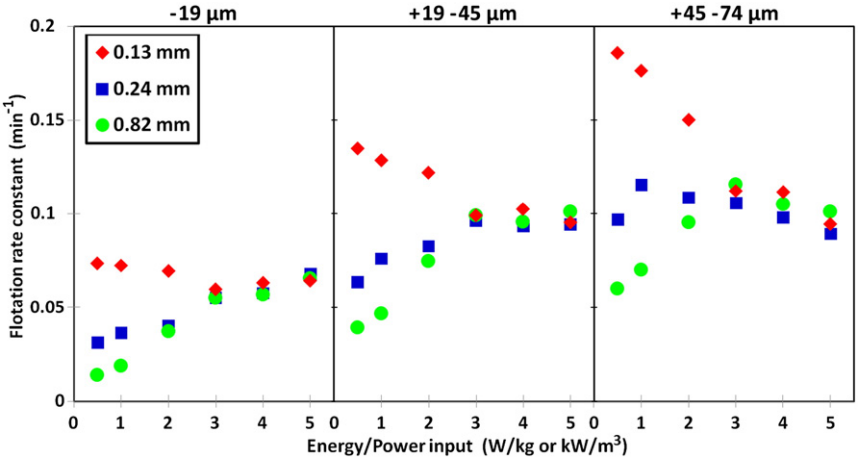

Fig. 7. Flotation rate constant versus energy input for three particle size classes, all bubble sizes and a moderate collector dosage.

improve the flotation of fine particles (−19 μm). This is probably due to quartz being less hydrophobic than the sulphide minerals, resulting in increased bubble-particle detachment for the smaller bubbles. For the two larger bubble sizes, increasing energy input leads to a steady increase in the flotation rate constant for fine particles (−19 μm) and optimal energy inputs for the intermediate (+19–45 μm) and coarse particles (+45–74 μm). The optimal energy input for the intermediate particles is in the vicinity of 4 to 5 W/kg, which is considerably higher than that the sulphide minerals in a comparable size range. This is probably due to quartz having a much lower density than the sulphide minerals, resulting in significantly decreased bubble-particle detachment at higher energy inputs.

5. Conclusions

This study investigated the effect of energy/power input on the flotation of three sulphide minerals (galena, pyrite & pentlandite) and three oxide minerals (apatite, hematite & quartz) in an oscillating grid flotation cell (OGC). From this study one may conclude that the effect of energy/power input on the flotation rate is strongly dependent on the mineral type, particle size, bubble size and collector dosage. Flotation rates for the sulphide minerals are generally higher than those for the oxide minerals. Flotation rates generally increase with increasing particle size, decreasing bubble size and increasing collector dosage, as is commonly found in the literature. Increasing energy input generally leads to an increase in the flotation rate for finer particles, an optimum flotation rate for more moderate particles and a decrease in the flotation rate for coarser particles. The optimum in the flotation rate for the sulphide minerals is at a lower energy input than that for the oxide minerals. The increases/decreases in the flotation rate with increasing energy/power input are very large, indicating that this is an important parameter in flotation.

Acknowledgements

The authors would like to thank the Australian Mineral Industries Research Association (AMIRA) (P9P project) for supporting this research.

References

Ahmed, N., Jameson, G., 1985. The effect of bubble-size on the rate of flotation of fine particles. Int. J. Miner. Process. 14, 195–215.
Anderson, C., Harris, M.C., Deglon, D.A., 2009. Flotation in a novel oscillatory baffled column. Miner. Eng. 22, 1079–1087.
Bache, D.H., Rasool, E., 2001. Characteristics of turbulence in a multigrid mixer. Chem. Eng. J. 83, 67–78.
Brunk, B.K., Koch, D.L., Lion, L.W., 1998. Observations of coagulation in isotropic turbulence. J. Fluid Mech. 371, 81–107.
Changunda, K., Harris, M.C., Deglon, D.A., 2008. Investigating the effect of energy input on flotation kinetics in an oscillating grid flotation cell. Miner. Eng. 21, 924–929.
Cowburn, J., Harbort, G., Manlapig, E., Pokrajcic, Z., 2006. Improving the recovery of coarse coal particles in Jameson cell. Miner. Eng. 19, 609–618.
Deglon, D.A., 1998. A hydrodynamic investigation of fine particle flotation in a batch flotation cell PhD Thesis Department of Chemical Engineering, University of Cape Town.
Deglon, D., 2002. A novel attachment — detachment kinetic model. Flotation and Flocculation — From Fundamentals to Applications, Hawaii.
Deglon, D.A., 2005. The effect of agitation on the flotation of platinum ores. Miner. Eng. 18 (8), 839–844.
De-Silva, I.P.D., Fernando, H.J.S., 1994. Oscillating grids as a source of nearly isotropic turbulence. Phys. Fluids 6, 2455–2464.
Diaz-Penafiel, P., Dobby, G., 1994. Kinetic studies in flotation columns: bubble size effect. Miner. Eng. 7, 465–478.
Huppert, H.E., Turner, J.S., Hallworth, M.A., 1995. Sedimentation and entrainment in dense layers of suspended particles stirred by an oscillating grid. J. Fluid Mech. 289, 263.
Herlina, Jirka, G.H., 2008. Experiments on gas transfer at the air–water interface induced by oscillating grid turbulence. J. Fluid Mech. 594, 183–208.
Jordan, C.E., Spears, D.R., 1990. Evaluation of a turbulent flow model for fine-bubble and fine-particle flotation. Miner. Process. Extr. Metall. Rev. 7, 65–73.
Koh, P.T.L., Schwarz, M.P., 2003. CFD modelling of bubble–particle collision rates and efficiencies in a flotation cell. Miner. Eng. 16, 1055–1059.
Massey, W.T., Harris, M.C., Deglon, D.A., 2012. The effect of energy input on the flotation of quartz in an oscillating grid flotation cell. Miner. Eng. 36–38, 145–151.
McDougall, T.J., 1979. Measurements of turbulence in a zero-mean-shear mixed layer. J. Fluid Mech. 94, 409–431.
Mokgethi, B., 2010. The Effect of Energy Input on Precipitation in an Oscillating Grid Reactor MSc Thesis Department of Chemical Engineering, University of Cape Town.
Newell, R., Grano, S., 2006. Hydrodynamics and scale up in Rushton turbine flotation cells: part 2 — flotation scale-up for laboratory and pilot cells. Int. J. Miner. Process. 81, 65–78.
Nguyen, A.V., George, P., Jameson, G.J., 2006. Demonstration of a minimum in the recovery of nanoparticles by flotation: theory and experiment. Chem. Eng. Sci. 61 (8), 2494–2509.
Nonaka, M., Inoue, T., Imaizumi, T., 1982. A micro-hydrodynamic flotation model and its application to the flotation process. Proceedings XIV International Mineral Processing Congress, Toronto.
Orlins, J., Gulliver, J., 2003. Turbulence quantification and sediment resuspension in an oscillating grid chamber. Exp. Fluids 34, 662–677.
Öteyaka, B., Soto, H., 1995. Modelling of negative bias column for coarse particles flotation. Miner. Eng. 8, 91–100.
Pushkarova, R.A., Horn, R.G., 2008. Bubble–solid interactions in water and electrolyte solutions. Langmuir 24 (16), 8726–8734.
Pyke, B., Fornasiero, D., Ralston, J., 2003. Bubble particle heterocoagulation under turbulent conditions. J. Colloid Interface Sci. 265, 141–151.
Saint Amand, J., 1999. Hydrodynamics of deinking flotation. Int. J. Miner. Process. 56, 277–316.
Schubert, H., 1999. On the turbulence-controlled microprocesses in flotation machines. Int. J. Miner. Process. 56, 257–276.
Schubert, H., 2008. On the optimization of hydrodynamics in fine particle flotation. Miner. Eng. 21, 930–936.
Schubert, H.J., Bischofberger, C., 1978. On the hydrodynamics of flotation machines. Int. J. Miner. Process. 5, 132–142.
Schulze, J.H., 1993. Flotation as a heterocoagulation process: possibilities of calculating the probability of flotation. In: Dobias, B. (Ed.), Coagulation and Flocculation and Applications. Dekker, New York, pp. 321–353.
Sherrell, I., Yoon, R.H., 2005. Development of a turbulent flotation model. Centenary of Flotation Symposium, Brisbane.
Tojo, K., Miyanami, K., Minami, I., Yano, T., 1979. Power dissipation in a vibrating disc column. Chem. Eng. J. Biochem. Eng. J. 17, 211–218.
Yoon, R., Luttrell, G., 1986. The effect of bubble size on fine coal flotation. Coal Prep. 2, 179–192.